Alma Mater Studiorum Università di Bologna
Archivio istituzionale della ricerca

A Comprehensive Investigation on the Accuracy of Electrical Measurement of Transport Current AC Losses in HTS Tapes

(Article begins on next page)

22 November 2024

A comprehensive investigation on the accuracy of electrical measurement of transport current AC losses in HTS tapes

M. Breschi, A. Musso, G. Pasini and P. L. Ribani

Abstract —The measurement of transport current AC losses in HTS tapes with the electric method has been extensively discussed in the literature. It is well known that the configuration of the circuit used to acquire the voltage signal can affect the measured losses, potentially leading to inaccurate results. To reduce this undesired effect, the rectangular circuit arrangement which is widely adopted involves twisting the pair of voltage taps at a given distance from the tape middle axis. However, the explanations reported in the literature to identify the correct distance are not fully exhaustive, and an alternative interpretation is here described.

Moreover, given that the conventional voltage taps arrangement creates a significant circuit area to which electromagnetic noise can be linked, an alternative configuration is proposed, aiming to reduce the linked flux.

This work presents a theoretical analysis to quantify the impact of the measurement circuit configuration on the losses. To ensure clarity, the model equations involved are derived step-by-step. The numerical results are applied to a thorough investigation on the accuracy of the AC losses measured on a sample tape, at different frequencies and current amplitudes. Both the conventional and the alternative arrangements are studied, varying their main geometrical parameters, at the same operating conditions. The correction terms are then applied to the measurement results, highlighting the advantages and drawbacks of the different configurations.

Index Terms —AC losses, High Temperature Superconductors, Coated conductors, Electromagnetic methods.

I. INTRODUCTION

Losses in alternate current applications are a well-known issue of superconducting devices. They must be carefully taken into account when designing a superconducting device working with time-varying currents and/or magnetic fields, since they strongly impact the overall losses and can affect the operating limits of the system [1 – 5]. Often, the analysis starts at the tape level, involving straight High Temperature Superconducting (HTS) tapes. Despite their AC losses are generally lower than those generated in a complex device, their simpler geometries allow a more detailed analysis of the AC loss phenomena and a straightforward comparison between different tape architectures [6]. However, their measurement is not trivial, due to the small magnitude of the quantities involved, especially for short tape samples. The experimental methods are generally classified in three main types: calorimetric, magnetic and electrical. The calorimetric techniques generally depend on the estimation of the amount of coolant evaporating due to the power dissipation, or are based on the use of thermocouples to assess temperature variations of bodies with a known thermal capacitance. They are insensitive to electromagnetic noise, but require an accurate calibration of the experimental setup to achieve a sufficient reliability [7 – 10]. On the other hand, magnetic and electric techniques (often referred to as electromagnetic methods) are faster and have a greater sensitivity; despite this, they are affected by electromagnetic noise. The magnetic methods rely on the measurement of the in-phase component of the voltage signal acquired from pick-up coils, which can be placed around the conductor, thus avoiding contacts and soldering, in order to measure magnetization losses [11 – 13]. This work focuses on the electric methods, which are based on the acquisition of the current and voltage signals from the sample, using an AC four-terminal technique with voltage taps soldered directly on the tape [14 – 19].

The measurement of the voltage signal is usually more difficult than that of the current (although ensuring a simultaneous acquisition of both signals is not trivial), at least at the single tape level. In fact, the expected voltage signal has a small amplitude and its component in phase with the AC transport current can easily be hidden by the electromagnetic noise linked to the voltage measurement circuit [20]. Theoretically, to reduce this problem, the area of the loop formed by the voltage circuit should be decreased. However, for the correct measurement of transport current AC losses in HTS tapes, a counter-intuitive approach must be considered, which is described in the literature as follows. It has been recognized that the losses do not arise solely due to the flux inside the conductor, but they also depend on how the flux outside the sample is affected by the presence of the superconductor [21]. Conductors having non-circular cross-section produce an asymmetric distribution of magnetic flux outside their surface, as in the case of tapes with a high aspect ratio [22 – 24]. This implies that the voltage signal induced by the flux linked with the measurement circuit has a component in

M. Breschi, A. Musso, G. Pasini and P. L. Ribani are with the Department of Electrical, Electronic and Information Engineering, of the University of Bologna, 40136 Bologna, Italy (e-mail: andrea.musso3@unibo.it).

phase with the current [25], and therefore it gives a loss contribution that must be taken into account [26]. It follows that the distance from the tape at which the signal wires are twisted together determines the area of the measurement loop (proportional to the linked flux) and thus the measured losses [27 – 30]. Theoretically, in the presence of an infinitely long tape, to make the measurements independent of the circuit geometry, the two signal wires should be brought to an infinite distance from the tape before twisting them, so that the flux lines are circular, as in the case of a cylindrical conductor [31]. This contrasts to the need to reduce the area for external noise linking; a compromise distance must be found to account for both requirements. To achieve this task, different configurations for the voltage circuit have been proposed in the literature.

The most adopted one is the *rectangular loop* arrangement (referred to as the *conventional* arrangement, in the following), which involves soldering the voltage taps onto the surface of the tape, at a given distance from each other. Then both wires are brought to a distance from the tape middle axis equal to 3 times the half-width of the tape, parallel to its main face, before twisting them together [24, 28, 32 – 34]. However, in other references this parameter is identified as 3 times the entire width of the tape [13, 21, 26, 35, 36]; these inconsistencies indicate that this topic, although treated in the literature, has not yet reached a consensus in the scientific community. In any case, the explanation for this widely used rule of thumb is not fully exhaustive in the literature. It mainly relies on empirical approaches, while there are few comparisons between different experimental methods (electromagnetic and calorimetric) [14, 16, 19, 37, 38] or between experimental and numerical models that quantify the impact of different circuit geometries [21, 24 – 26 28]. The latter are generally applied to BSCCO tapes other than to coated conductors.

A different arrangement is called the *spiral voltage lead loop*, which consists in placing the two signal wires in a spiral path around the tape before being twisted. The path is realized on a cylindrical surface of constant radius (whose value has no impact on the measurement), at a constant pitch and with an integer number of turns [39]. This should reduce the linked electromagnetic noise and the resulting out-of-phase component of the acquired signal, as well as improving the system compactness [40 – 44]. An alternative arrangement, that aims to solve the same problem, is called *8 shaped pick-up loop* [45]. In this case, the two voltage wires are brought to a distance at least equal to 3 times the half-width of the tape from its middle axis, parallel to its main face, but in opposite directions. Then, both wires are led parallel to the tape length, towards each other, to the midpoint between the two voltage taps. Finally, one wire is joined to the other passing perpendicular to the tape length, and the two are twisted together. This forms an "8 shaped" loop consisting of two parts having opposite orientation with respect to the direction of the magnetic flux lines outside the tape. Since the self-field is assumed to be symmetric with respect to the plane passing through the tape axis and perpendicular to its broad face, this configuration should properly reduce the external flux linkage.

The aforementioned configurations may have some advantages over the rectangular loop, but are more complex to realize.

Furthermore, given that conventional voltage taps (soldered or pressed onto the tape) can damage the superconductor and affect its local thermal stability, it has been proposed to place the voltage taps outside the current leads [46]. Then, the losses generated in the conventional copper blocks used as current leads can be numerically estimated and subtracted from the measured values, in order to discern the losses in the tape alone. This arrangement seems suited for particular applications where the magnitude of the AC losses in the superconductor is comparable to those produced in the copper.

Finally, other works claim that, when analyzing the AC losses generated in tapes located inside stacks or placed side by side, the use of the *edge voltage leads* con be convenient, in which the voltage taps are soldered to one tape edge and twisted together without distancing them from the conductor [47, 48].

In this paper, the impact of the voltage taps configuration on the measured transport current AC losses is determined through a theoretical and experimental analysis, with particular regard to the distance from the middle axis at which the signal wires are twisted in the conventional arrangement. The proposed numerical method adopts an alternative approach compared to the literature, based on the *A-V* formulation [49], and it allows to calculate the correction term to be applied to the experimental results, in order to improve the accuracy of the measurement.

Moreover, the investigation accounts for all materials composing the HTS coated conductor, and not only its superconducting layer. Given that the rectangular loop configuration forms a circuit with a non-negligible area, the measurements could be heavily affected by electromagnetic noise. To reduce the noise, a different configuration for measuring the voltage signal is also presented, and compared to the conventional arrangement.

Finally, an experimental campaign is conducted on a tape sample, carrying out electric measurements with different setup geometries and operating conditions, in terms of transport current amplitude and frequency. The correction terms are then applied and the results are compared with those obtained with analytic formulations and numerical models.

Indeed, this work proposes a novel algorithm to correct the measurement results, which however requires the availability of a numerical model. The aim of the work is therefore mainly to provide a comprehensive description of the measurement methodologies described in the literature and to quantitatively assess their inherent accuracy in the measurement of transport current AC losses in HTS tapes.

II. DETERMINATION OF THE CORRECTION TERM FOR DIFFERENT SETUP CONFIGURATIONS

This section describes the theoretical passages and the equations adopted to investigate the impact of the voltage circuit arrangement on the measurement of transport current AC transport current $I_{Tot} = I_{Amp} \sin(2\pi f t)$, with frequency f. The tape has a finite length L, and is directed along the z-axis of the Cartesian reference system, as shown in Fig. 1.
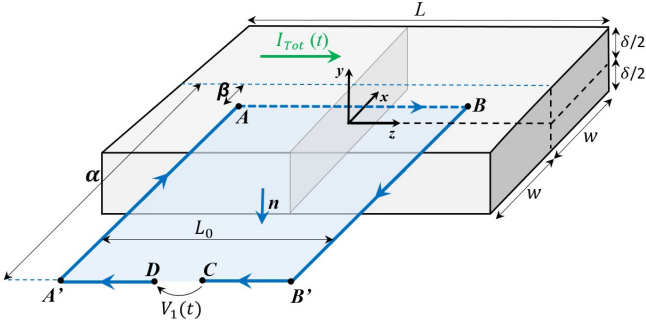
Fig. 1. Scheme of the conventional loop arrangement for voltage measurement, applied to a straight tape. The figure is not in scale

The half-width and the thickness of the tape are indicated as w and δ, respectively. The power $p(t)$ dissipated at the time instant t, in the central portion of the tape of length L_0, included between the voltage taps (regardless of the measurement setup), can be computed as:

$$p(t) = \int_{-\frac{L_0}{2}}^{\frac{L_0}{2}} \int_{-\frac{\delta}{2}}^{\frac{\delta}{2}} \int_{-w}^{w} \boldsymbol{E}(x,y,z,t) \cdot \boldsymbol{J}(x,y,z,t) dx dy dz \quad (1)$$

where $\boldsymbol{E}$ is the electric field vector and $\boldsymbol{J}$ is the transport current density vector.

With the same approach used in [50] for the A-V formulation, the following assumptions are made for the central portion of the tape between the voltage taps:

$$\begin{aligned}
\boldsymbol{E}(x,y,z,t) &= E(x,y,t)\,\boldsymbol{k} \\
\boldsymbol{J}(x,y,z,t) &= J(x,y,t)\,\boldsymbol{k} \\
\boldsymbol{A}(x,y,z,t) &= A(x,y,t)\,\boldsymbol{k} \\
V(x,y,z,t) &= V(z,t)\,\boldsymbol{k}
\end{aligned} \quad (2)$$

where V and A are the scalar electric potential and the magnetic vector potential respectively, and $\boldsymbol{k}$ is the unit vector directed along the z-axis. These hypotheses correspond to assuming that the central portion of the tape is at a sufficient distance from the tape ends, so that the distribution of the vectors $\boldsymbol{J}$, $\boldsymbol{A}$ and $\boldsymbol{E}$ is independent of the z-coordinate, and these vectors are all directed along the z-axis. The last equation corresponds to the assumption of equipotential cross-sections of the x-y planes.

The electric field can then be expressed as a function of the scalar and vector potentials. Applying the assumptions reported in (2), gives:

$$E(x,y,t) = -\frac{\partial V}{\partial z}(t) - \frac{\partial A}{\partial t}(x,y,t) \quad (3)$$

where it has been assumed that the derivative of V with respect to the z-coordinate is independent of z, consistently with the hypothesis that the electric field does not depend on z in the middle position of the tape.

Combining (3) and (1) and performing the integration along the z-coordinate, according to the simplifying assumptions made, yields:

$$p(t) = -L_0 \int_{-\frac{\delta}{2}}^{\frac{\delta}{2}} \int_{-\frac{w}{2}}^{\frac{w}{2}} \left(\frac{\partial V}{\partial z}(t) J(x,y,t) \right) dx dy -$$

$$L_0 \int_{-\frac{\delta}{2}}^{\frac{\delta}{2}} \int_{-\frac{w}{2}}^{\frac{w}{2}} \left(\frac{\partial A}{\partial t}(x,y,t) J(x,y,t) \right) dx dy =$$

$$= V_{AB}(t) I_{Tot}(t) + p_A(t) \quad (4)$$

$$with \begin{cases}
V_{AB}(t) = -L_0 \dfrac{\partial V}{\partial z}(t) \\[2mm]
I_{Tot}(t) = \displaystyle\int_{-\frac{\delta}{2}}^{\frac{\delta}{2}} \int_{-w}^{w} J(x,y,t)\, dx dy \\[2mm]
p_A(t) = -L_0 \displaystyle\int_{-\frac{\delta}{2}}^{\frac{\delta}{2}} \int_{-w}^{w} \dfrac{\partial A}{\partial t}(x,y,t) J(x,y,t) dx dy
\end{cases}$$

where V_{AB} is the voltage difference between the points A and B on the tape surface corresponding to the voltage taps soldering, and p_A is the loss contribution due the non-conservative part of the electric field. It is worth noting that the term $\partial V/\partial z\,(t)$ has been taken out of the integral, since it does not depend on the x and y coordinates, as assumed in (2).

Therefore, the transport current AC losses (P_{AC}) correspond to the average value in a period of the dissipated power. The averaging is applied to the expression in (4), considering that $\langle p_A(t) \rangle = 0$, as it is demonstrated in the *Appendix*. Then, dividing by the term L_0 to obtain the average power dissipation per unit length, gives:

$$P_{AC} = \frac{1}{L_0}\langle p(t) \rangle = \frac{1}{L_0}\langle V_{AB}(t) I_{Tot}(t) \rangle \qquad \left[\frac{W}{m}\right] \quad (5)$$

Using conventional current transducers (*e.g.* a shunt resistor placed in series with the tape sample), the current $I_{Tot}(t)$ can be directly measured without affecting the losses calculated through (5). Conversely, the voltage signal that is detected with the voltmeter connected to the couple of wires soldered on the tape, called V_1 (what the user acquires), does not exactly coincide with the voltage V_{AB} (the voltage difference between points A and B onto the tape). This difference is affected by the configuration of the voltage circuit, as already mentioned in the literature. However, quantifying this difference is not trivial; it is therefore useful to develop the corresponding theory in depth to understand possible ways to improve the measurement, also by applying suitable corrections to the measured voltage.

A. Conventional rectangular loop arrangement

This configuration corresponds to the one displayed in Fig. 1. The voltage taps are soldered to the tape surface, at a distance β from the tape middle axis, at points A and B having coordinates $(\beta, \delta/2, \pm L_0/2)$. The wires are brought to a generic distance α from the tape middle axis, up to the points A' and B', having the same y coordinate as A and B. In the conventional configuration, $\alpha \geq w > \beta$. Then, the wires are twisted together and connected to the voltmeter channel, at points C and D,

where the signal $V_1(t)$ is acquired. The relation between V_1 and V_{AB} can be determined by applying the integral form of the Faraday's law to the closed circuit represented in Fig. 1 by the blue solid line (indicated as C_1), including the dashed line connecting points A and B. The integration yields:

$$\oint_{C1} \boldsymbol{E} \cdot \boldsymbol{dl} = \int_A^B \boldsymbol{E} \cdot \boldsymbol{dl} + \int_B^C \boldsymbol{E} \cdot \boldsymbol{dl} + \int_C^D \boldsymbol{E} \cdot \boldsymbol{dl} + \\ + \int_D^A \boldsymbol{E} \cdot \boldsymbol{dl} = -\frac{d\emptyset_{C1}}{dt}(t) \tag{6}$$

where $\emptyset_{C1}$ is the flux of the magnetic flux density through the surface (in light-blue in Fig. 1) bounded by C_1 and having its normal unit vector perpendicular to the travel direction of the circuit in accordance to the right-hand rule. In this first analysis, any external electromagnetic noise is neglected and the flux depends only on the current flowing in the conductor.

It is worth noting that, under the hypotheses of this study, the system shown in Fig. 1 is symmetric with respect to the *y-z* plane. Therefore, the passages reported in the following for positive α and β values, lead to the same results also when these parameters are both negative.

Due to the large internal impedance of the voltmeter, the currents flowing in the wires corresponding to the portions of circuit *B-C* and *D-A* are negligible, and thus their contribution can be ignored.

As already stated, the contribution of the segment *C-D* is equal to $-V_1(t)$, where the sign is in accordance with the integration extremes.

Moreover, introducing (3) into the term which refers to the segment *A-B*, this contribution can be expressed as:

$$\int_A^B \boldsymbol{E} \cdot \boldsymbol{dl} = -\int_A^B \frac{\partial V}{\partial z}(z,t)\,dz - \int_A^B \frac{\partial A}{\partial t}\left(\beta,\frac{\delta}{2},t\right)dz = \\ = V_{AB}(t) - L_0 \frac{\partial A}{\partial t}\left(\beta,\frac{\delta}{2},t\right) \tag{7}$$

Substituting in (6) the contribution given by each portion of C_1, and isolating the term $V_1(t)$, yields:

$$V_1(t) = V_{AB}(t) + \varepsilon_c(\alpha,t) \\ \varepsilon_c(\alpha,t) = -L_0 \frac{\partial A}{\partial t}\left(\beta,\frac{\delta}{2},t\right) + \frac{d\emptyset_{C1}}{dt}(t) \tag{8}$$

where $\varepsilon_c(\alpha,t)$ is the term expressing the difference between the quantities $V_{AB}(t)$ and $V_1(t)$. It is worth noting how this term depends both on the linked flux, which can be lowered by reducing the area bounded by C_1 (in practice, it cannot be null since the signal wires always enclose a given area), and on the term $-L_0(\partial A/\partial t)$, which cannot be avoided when applying electrical methods to measure AC losses in HTS tapes. The dependence on the parameter α will be clarified in the following passages.

Then, the term $\emptyset_{C1}$ in (8) can be expressed by means of the Stokes' theorem, as the circulation of the vector potential along the line C_1. It is convenient to split C_1 into two parts: the first section corresponds to the segment *A-B*, while the second one corresponds to the rest of the circuit (*B-B'-C-D-A'-A*), called C_{1bis}.

$$\emptyset_{C1}(t) = \int_A^B \boldsymbol{A} \cdot \boldsymbol{dl} + \int_{C_{1bis}} \boldsymbol{A} \cdot \boldsymbol{dl} = \\ = L_0 A\left(\beta,\frac{\delta}{2},t\right) + \int_{B'}^{A'} A\left(\alpha,\frac{\delta}{2},z,t\right)dz \tag{9}$$

In (9), the vector potential has been taken out of the first integral as it is considered independent of the *z*-coordinate in the conductor region. Moreover, with a certain level of approximation, the hypothesis for which the vector potential has only a *z*-component can be assumed valid for the whole measurement circuit, and not only in the tape region. It follows that the only portion of C_{1bis} that gives a contribution in (9) is the line *B'-A'*, since for the other segments the vectors $\boldsymbol{A}$ and $\boldsymbol{dl}$ are perpendicular. The assumptions reported in (2) do not automatically apply outside the tape; therefore, the vector potential along the line *B'-A'* also depends on the *z* coordinate.

Inserting (9) into (8), yields:

$$V_1(t) = V_{AB}(t) - L_0 \frac{\partial A}{\partial t}\left(\beta,\frac{\delta}{2},t\right) + L_0 \frac{\partial A}{\partial t}\left(\beta,\frac{\delta}{2},t\right) + \\ + \int_{B'}^{A'} \frac{\partial A}{\partial t}\left(\alpha,\frac{\delta}{2},z,t\right)dz = V_{AB}(t) + \varepsilon_c(\alpha,t) \\ \varepsilon_c(\alpha,t) = \int_{B'}^{A'} \frac{\partial A}{\partial t}\left(\alpha,\frac{\delta}{2},z,t\right)dz \\ = -\int_{-\frac{L_0}{2}}^{\frac{L_0}{2}} \frac{\partial A}{\partial t}\left(\alpha,\frac{\delta}{2},z,t\right)dz \tag{10}$$

where the integration extremes in the term $\varepsilon_c(t)$ have been substituted with the *z*-coordinates of the points *A'* and *B'*.

A first conclusion that can be drawn from (10), is that the voltage signal (as well as the current one) does not depend on the parameter β. Therefore, in the conventional configuration, the position at which the wires are soldered to the tape does not affect the measured losses.

Finally, introducing (10) in (5), yields:

$$P_{AC} = \frac{1}{L_0}\langle V_1(t)I_{Tot}(t) - \varepsilon_c(\alpha,t)\,I_{Tot}(t)\rangle = \\ = \frac{1}{L_0}\langle V_1(t)I_{Tot}(t)\rangle + \eta_c \tag{11} \\ \eta_c(\alpha) = \frac{1}{L_0}\left\langle \left(\int_{-\frac{L_0}{2}}^{\frac{L_0}{2}} \frac{\partial A}{\partial t}\left(\alpha,\frac{\delta}{2},z,t\right)dz\right)I_{Tot}(t)\right\rangle$$

where η_c represents the correction term to be applied to the measurement results obtained with the conventional rectangular configuration (in W/m) to account for the difference between the voltmeter measurement V_1 and the voltage V_{AB} needed for the losses assessment. Neglecting this term without having

properly designed the voltage circuit configuration would lead to an incorrect estimation of the AC losses in the tape.

B. Techniques for the reduction of the voltage difference term

The following approach can be followed to cancel or reduce the term η_c, thus making the measurements independent of the voltage circuit configuration. First, it is necessary to evaluate whether the assumptions listed in (2) can be extended to a certain distance from the conductor. If this extension is acceptable, the integral in (11) can easily be solved, as the integrand $\partial A / \partial t$ is independent of the z-coordinate:

$$\eta_c(\alpha) = \frac{1}{L_0} \left\langle L_0 \frac{\partial A}{\partial t}\left(\alpha, \frac{\delta}{2}, t\right) I_{Tot}(t) \right\rangle \qquad (12)$$

In order for $\eta_c(\alpha)$ to be equal to zero, the average over the period in (12) has to be null. Neglecting the case in which one of the quantities is zero, this condition is verified only if the whole term within the mean is periodic with a null mean. For this to be the case, the vector potential should depend on the total current only, and not on the current distribution inside the tape, as follows:

$$A\left(\alpha, \frac{\delta}{2}, z, t\right) = C(\alpha) I_{Tot}(t) \qquad (13)$$

where $C(\alpha)$ is a constant (for simplicity of notation only the dependence on α is indicated).

If (13) is valid, then the whole term to be averaged in time in (12) corresponds to a sinusoidal function with a null mean. This assumption is verified for a conductor having a circular cross-section, where, due to the cylindrical symmetry, for every value of α the field only depends on the total current. This is generally not valid for a tape having a high aspect ratio, in which the current density is not uniformly distributed. However, it is relevant for this work to investigate whether there are values of α allowing to adopt (13) also for tapes. For instance, it is clear that moving sufficiently away from the conductor surface (*i.e.* increasing α), the internal current distribution becomes less relevant. At an infinite distance from the tape, the same condition existing for a cylindrical conductor can also be applied for a tape, which corresponds to the conclusions reported in the literature [21]. In practical terms, a value of α large enough to verify (13) should be found, which would then lead to:

$$\eta_c(\alpha) = \left\langle C(\alpha) \frac{dI_{Tot}(t)}{dt} I_{Tot}(t) \right\rangle \approx 0 \qquad (14)$$

where (14) is exactly null only if α is infinite. It is reasonable to assume that even at lower α values, the dependence of the vector potential on the internal current distribution becomes progressively less relevant as α increases, and thus η_c approaches zero.

This approach is correct only if it is possible to find a value of α large enough to satisfy (14), while keeping the assumptions (2) valid. In fact, these two assumptions are in contrast with each other: if α increases, considering the vector potential to be independent of the z-coordinate becomes problematic, since it implies that the tape is still sufficiently long as compared to the

rest of the measurement circuit. Moreover, as α increases, also the area bounded by C_1 widens. This enhances the undesired voltage signal generated in the measurement circuit by the flux linkage of electromagnetic noise, taken into account by the term $\emptyset_{C1}$, that can have a relevant impact in practical cases.

As reported in the introduction, many works reported in the literature deal with the optimal α value to be used in the rectangular arrangement, in order to reduce the linked flux while guaranteeing the validity of the simplifying hypotheses. In the following sections, (14) is solved numerically for some relevant case studies, in order to quantify the impact of the circuit arrangement for different values of α.

C. Alternative arrangement for the minimization of the electromagnetic noise

An alternative configuration for the voltage measurement circuit is proposed in this section. The purpose of this new arrangement is to reduce the electromagnetic noise with respect to the rectangular configuration, without excessively complicating the circuit.

In fact, the external flux is hard to compensate during the post-processing of the signals. The parameter η_c, for example, does not take into account this contribution, which therefore may strongly affect the measured losses. This is particularly important when the experiments are carried out without an appropriate shielding from external electromagnetic noise, or when the amplitude of the transport current is much smaller than the critical current of the tape, and therefore the magnitude of the V_{AB} signal is small.

Compared to the conventional rectangular configuration, the alternative arrangement includes an auxiliary voltage measurement circuit, depicted as a red solid line in Fig.2, and hereafter labelled as C_2.

The first circuit (corresponding to the blue solid line in Fig. 2, equivalent to C_1) is identical to the rectangular loop described in the previous section, except that, in this case, the area of the loop is kept as small as possible. Ideally, the line A'-B' coincides with the line A-B. In practice, a small area is inevitable; in Fig. 2, the loop dimensions are magnified to make it evident. On the other hand, C_2 is arranged so as to follow as much as possible the shape of C_1. This can be achieved by the use of non-twisted ribbon cables. The purpose of this compensation circuit is to reduce the electromagnetic noise of the acquired
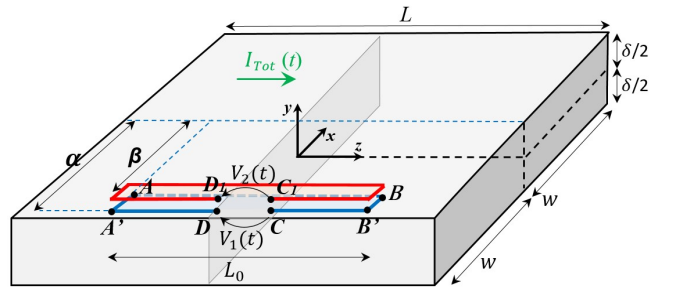

Fig. 2. Scheme of the alternative arrangement for the voltage measurement and the minimization of the electromagnetic noise, applied to a straight tape. The figure is not in scale.

signal. The wires of C_2 are not soldered onto the tape but they are short-circuited together. These additional wires are connected to the terminals C_1 and D_1 of the second channel of the voltmeter. The corresponding voltage signal is acquired simultaneously to the first measurement and indicated as $V_2(t)$.

For what concerns C_1, the same passages which led to the definition of $V_1(t)$ in (10) are also valid for this arrangement. To define $V_2(t)$ instead, the Faraday's law is applied to C_2, as already done to retrieve (6). In this case, the only part of the closed curve which results in a non-null contribution is the segment C_1-D_1, which gives exactly $V_2(t)$ (except for the sign). It results:

$$\oint_{C2} \boldsymbol{E} \cdot \boldsymbol{dl} = \int_{C_1}^{D_1} \boldsymbol{E} \cdot \boldsymbol{dl} = -V_2(t) = -\frac{d\emptyset_{C2}}{dt}(t) \qquad (15)$$

where $\emptyset_{C2} = \emptyset_{C1}$ is the same flux appearing in (8), considering that both circuits have the same shape (in reality, a small difference exists between them).

Then, $V_2(t)$ is subtracted from $V_1(t)$, leading to the signal $V_{1-2}(t)$, which has the following expression:

$$V_{1-2}(t) = V_1(t) - V_2(t) = V_{AB}(t) + \varepsilon_a(\beta, t)$$
$$\varepsilon_a(\beta, t) = -L_0 \frac{\partial A}{\partial t}\left(\beta, \frac{\delta}{2}, t\right) \qquad (16)$$

where $\varepsilon_a(\beta, t)$ corresponds to the discrepancy between the quantities $V_{AB}(t)$ and $V_{1-2}(t)$. Compared to the conventional configuration, the voltage signal acquired depends in this case on the soldering locations of the voltage taps, but does not depend on the parameter α. It follows that the measured losses are independent of the distance at which the wires are twisted together, which can be set as small as possible. In the alternative arrangement, $\alpha \approx \beta \leq w$.

Finally, introducing (16) in (5), yields:

$$P_{AC} = \frac{1}{L_0} \langle V_{1-2}(t)I_{Tot}(t) - \varepsilon_a(\beta, t) I_{Tot}(t) \rangle =$$
$$= \frac{1}{L_0} \langle V_{1-2}(t)I_{Tot}(t) \rangle + \eta_a(\beta) \qquad (17)$$
$$\eta_a(\beta) = \frac{1}{L_0} \left\langle L_0 \frac{\partial A}{\partial t}\left(\beta, \frac{\delta}{2}, t\right) I_{Tot}(t) \right\rangle$$

where η_a represents the correction term to be applied to the measurements in the alternative arrangement (in W/m) to account for the discrepancy between the signal acquired from the two voltmeter channels, V_{1-2}, and the "correct" voltage, V_{AB}.

Even for this arrangement, it can reasonably be assumed that a value of β exists, for which the vector potential can be expressed as a linear and time-invariant function of the tape transport current, as was done in (13) for the conventional configuration. It follows:

$$\eta_a(\beta) = \left\langle K\left(\beta, \frac{\delta}{2}\right)\frac{dI_{Tot}(t)}{dt} I_{Tot}(t) \right\rangle \qquad (18)$$

where K has the same meaning as the term C in (13) and (14).

In the following sections, the correction terms η_c and η_a are numerically computed for a test case, to analyze their dependencies on the α and β parameters.

III. NUMERICAL ANALYSIS ABOUT THE CORRECTION TERMS

To carry out a parametric analysis, the equations for the calculation of the correction terms are implemented in a numerical model. The definitions of η_c and η_a, reported in (12) and (17) respectively, only differ for the dependence on α or β, both of which represent a distance from the tape middle axis. Therefore, the numerical implementation of the two parameters is identical, and thus only the one corresponding to η_c is described here.

First, the tape cross-section is discretized into N rectangular-shaped elements. This also includes the non-superconducting layers of the coated conductors, that are often neglected in modeling, but which can have a significant impact under certain operating conditions [48].

A. Numerical calculation of the correction terms

As a second step, the assumption made in (11) and (12) can be dropped, or rather its validity can be checked for practical cases. Thus, (12) can be written without assuming the vector potential as independent of the z-coordinate:

$$\eta_c(\alpha) = \langle\langle \frac{\partial A\left(\alpha, \frac{\delta}{2}, z, t\right)}{\partial t} I_{Tot}(t) \rangle_{time} \rangle_{z \in \left[\frac{-L_0}{2}, \frac{L_0}{2}\right]} \qquad (19)$$

where the mean along the z-axis is performed on N_z elements, uniformly distributed along the z-coordinate in the range from $-L_0/2$ to $L_0/2$.
Then, the following expression is adopted to numerically compute the derivative of the vector potential that appears in (19):

$$\frac{\partial A\left(\alpha, \frac{\delta}{2}, z, t\right)}{\partial t} = \sum_{j=1}^{N} K_j\left(\alpha, \frac{\delta}{2}, z\right)\frac{\partial J_j(t)}{\partial t}$$

$$K_j\left(\alpha, \frac{\delta}{2}, z\right) =$$

$$= \frac{\mu_0}{4\pi} Area_j \left| \ln\left(\sqrt{(\alpha - x_j)^2 + \left(\frac{\delta}{2} - y_j\right)^2 + (z - z')^2}\right.\right. \qquad (20)$$

$$\left. + (z - z') \right)\Bigg|_{\frac{L}{2}}^{-\frac{L}{2}}$$

where $Area_j$ indicates the area of each discretizing element and μ_0 is the vacuum permeability. The current densities in each discretizing element $Jj(t)$ can be numerically computed by means of any formulation conventionally adopted so solve Maxwell's equations [51 − 55].

In this work, an integral model based on the *A-V* formulation is selected to calculate the current densities and then estimate the power dissipated in the tape (*i.e.* the value independent of the measurement configuration), by means of (1). The model employed considers the electrical properties of the different layers of a coated conductor, adopting the power law for the superconducting layer. Details on the model are reported in [50].

In this work, the model is applied to the analysis of the *SuNAM SCN04* tape. The tape geometrical parameters are shown in Fig. 3 [56]; the buffer layer is neglected in the model, given its small thickness. The tape length (L) is set to 15 cm, and the distance between voltage taps (L_0) is set to 6 cm. The critical current (I_c) and *n-value* of the tape at 77 K (with a 1 μV/m criterion) correspond to 242 A and 43, respectively. The average in time is performed over the first period in which the power vs time curve reaches steady-state conditions, which normally occurs at the second period. The amplitude and frequency of the transport current are varied to check their relation with the correction terms. Hereafter, the amplitude of the transport current is expressed as a dimensionless ratio: $I_m = I_{Amp}/I_c$. For the conventional arrangement, η_c is computed for $\alpha \geq w$ (*i.e.* the line *A'-B'* should be distant from the tape middle axis), while for the alternative configuration, $\beta \leq w$ (*i.e.* the line *A-B* lies on the tape surface).

Fig. 4 reports the correction terms computed as a function of α or β, both divided by the half width of the *SuNAM SCN04* tape ($w = 2$ mm) to obtain a dimensionless quantity. Two frequencies are studied, 50 Hz and 1 kHz, as well as two current amplitudes, $I_m = 0.5$ (Fig. 4a) and $I_m = 0.9$ (Fig. 4b).
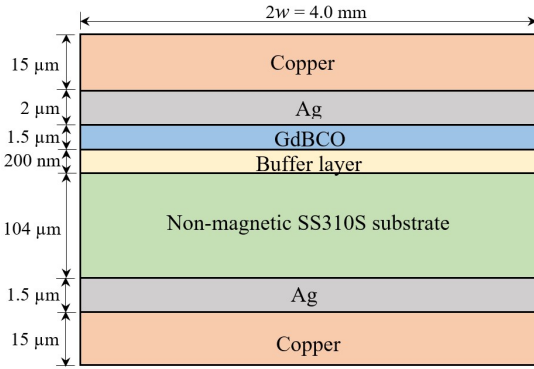
On the other hand, the correction term η_a exhibits a plateau at the center of the tape (both η_c and η_a are symmetric with respect to the tape center). Inside this region, η_a assumes positive values as it represents how much the AC losses measured in the alternative arrangement should be increased to converge to the correct value. Moving further to the tape sides, the η_a curve drops sharply to negative values, passing through a null value. For this unique point, which is current dependent and almost frequency independent, (18) is exactly verified. The existence of such value has never been mentioned in the literature, and it could present an advantage of the proposed alternative configuration, as it will be explained later in this section. Finally, for β very close to w, the η_a curve reverses its slope, increasing until it converges to the η_c curve, at $\alpha = \beta = w$. Moreover, just like the AC losses, both η_c and η_a rise as the frequency and/or the amplitude of the transport current increase.

In order to better quantify the impact of the circuit arrangement on the measured losses, it is convenient to present the correction terms η_c and η_a as a percentage of a reference value of losses ($P_{AC_{ref}}$), indicated as γ_c and γ_a, respectively:

$$\gamma_c(\alpha) = \left|\frac{\eta_c(\alpha)}{P_{AC_{ref}}}\right| \cdot 100 \; ; \; \gamma_a(\beta) = \left|\frac{\eta_a(\beta)}{P_{AC_{ref}}}\right| \cdot 100 \; [\%] \quad (21)$$

It is not possible to select an experimental curve of AC losses as the correct reference a priori. For example, with the

Fig. 3. Cross-section of the *SuNAM SCN04* tape. The figure is not in scale.

B. Results and discussion

For what concerns η_c, its values are always negative. Thus, in the rectangular arrangement, η_c indicates how much the measured AC losses must be reduced to converge to the correct value. As expected, the amplitude of η_c decays abruptly with increasing α. The curve reaches convergence for $\alpha = 3\,w$, and this distance is independent of both current amplitude and frequency. At convergence, η_c assumes negligible values, *i.e.* the measured AC losses are independent of the circuit arrangement. It is worth noting that the electromagnetic noise is not taken into account by η_c, but it is expected to increase with α.
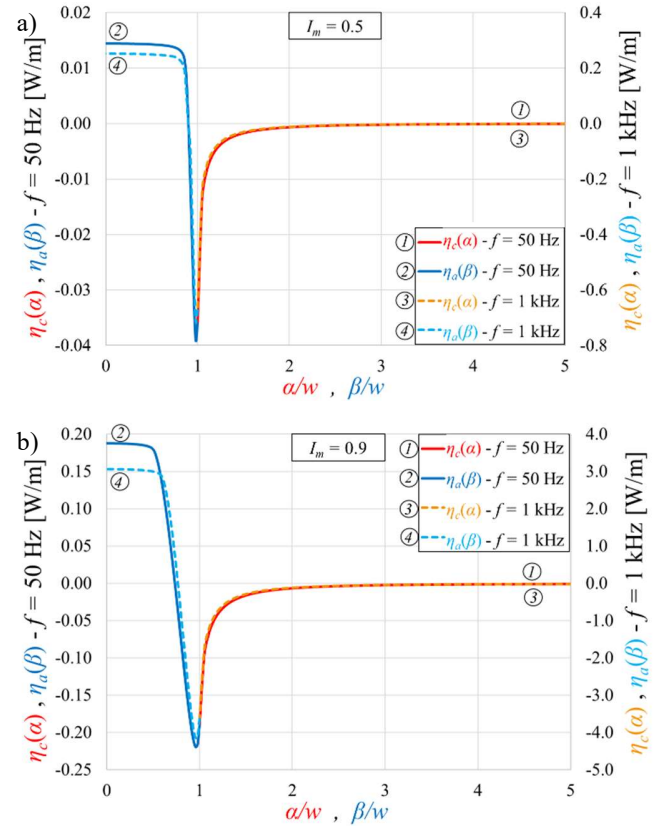

Fig. 4. Correction terms in W/m for (a) $I_m = 0.5$ and (b) $I_m = 0.9$, at 50 Hz (left axis) and 1 kHz (right axis), versus the parameters α and β.

conventional arrangement, even at an ideally infinite distance from the tape, the external electromagnetic noise could lead to results affected by a large error.

The aforementioned numerical model based on the *A-V* formulation [50] is considered reliable to accurately estimate the AC losses. Moreover, the model results are in excellent agreement with those of a different numerical method based on the *H*-formulation [57 –59], as well as with the experimental measurements [50, 55, 60, 61]. Notwithstanding some level of arbitrariness in the selection of the reference results, the following definitions and plots provide some guidance in the understanding of the impact of the correction on the accuracy of the measurement methodology adopted. Fig. 5 shows the parameters γ_c and γ_a, for the same cases displayed in Fig. 4.

As mentioned above, for $\alpha \geq 3\,w$, the losses measured with the rectangular arrangement coincide with the reference losses, as γ_c becomes negligible ($\gamma_c \approx 1.5\%$ at $\alpha = 3\,w$). This value corresponds to the one reported in various publications [24, 28, 32 – 34]. For the conventional configuration, reaching this threshold is crucial: γ_c increases exponentially when $\alpha < 3w$, and the experimental results tend to overestimate the reference value by a factor of up to 2.5. Moreover, γ_c results greater for higher I_m values but is not affected by the frequency: as the frequency increases, both the actual AC losses and the loss contribution due to the measurement system increase. If, for any reason, it is not possible to place the line *A'-B'* at a sufficient distance from the

tape middle axis, the accurate measurement of the α value becomes crucial, as the correction term varies abruptly over a very small distance. If this is not the case, the conventional configuration is the one that allows to relax more the precision criterion regarding the arrangement of the voltage circuit, as its loss contribution is negligible for any value of α greater than $3w$. However, this configuration requires to widen the circuit area, and thus it is convenient to remain close to this limit distance not to increase the linked electromagnetic noise.

For what concerns the parameter γ_a, there is an exactly null value in a point within the tape width. With reference to the *SuNAM SCN04* tape, at $I_m = 0.9$ the point is located at a distance from the tape middle axis equal to 1.5 mm, while for $I_m = 0.5$, this point moves closer to the tape sides, at $\beta = 1.8$ mm. The point location is only slightly affected by the frequency, especially at low current amplitudes. In correspondence of this point only, the measured losses are independent of the experimental setup and, differently from the conventional arrangement, the circuit area is considerably reduced (ideally null). This would lower (potentially cancel) the linked external noise, thus making the measurement more precise. However, the accuracy in the soldering of the voltage taps and in the determination of the value of β must be extremely high, especially for narrow tapes. In fact, in the immediate vicinity of the null point, γ_a increases abruptly: a small error of only 0.2 mm in the soldering compared to the null point leads to an increase in the contribution of the measurement circuit up to 250%, for the tested cases. As an example, a standard soldering covers a certain area of the tape surface and could never be punctual, thus making it more difficult to determine β exactly. The adoption of the alternative configuration can be practical if the voltage taps are soldered near the tape middle axis. In fact, in this central region there is a plateau in which the impact of the measurement circuit on the losses is almost constant.

It is worth noting that γ_a seems independent of the operating conditions, remaining around 100% for all cases (*i.e.* the measured losses must be doubled to obtain the correct value). The width of this plateau is larger for lower I_m, and appears to be slightly affected by the frequency. For the *SuNAM SCN04* tape, as long as β is less than 1 mm (thus identifying an area of 2 mm at the tape center), γ_a undergoes variations lower than 1% compared to the value assumed on the middle axis. This would allow to relax the precision criteria required in the alternative arrangement, while maintaining the advantage of a lower linked noise as compared to the conventional configuration.

Fig. 5. Correction terms as a percentage for (a) $I_m = 0.5$ and (b) $I_m = 0.9$, at 50 Hz (left axis) and 1 kHz (right axis), versus the parameters α and β.

IV. EXPERIMENTAL ANALYSIS ON THE APPLICATION OF THE CORRECTION TERMS

An experimental campaign was carried out to measure the transport current AC losses in the tape analyzed in this study. The *SuNAM SCN04* tape was tested on a rigid G10 straight support, immersed in liquid nitrogen bath. The description of the experimental setup developed to generate the AC current of variable amplitude and frequency, as well as the post-processing
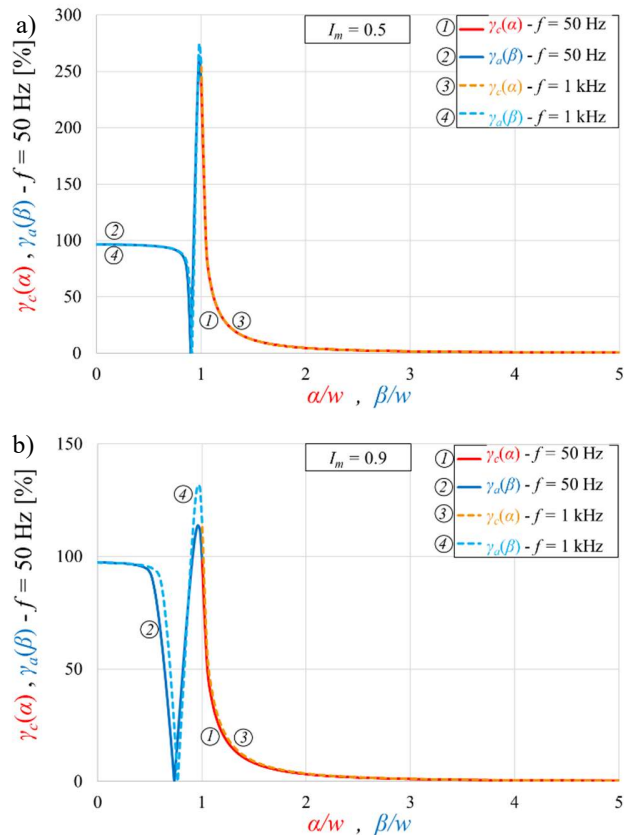
technique adopted to filter the harmonics of the transport current frequency from the acquired signals (regardless of the configuration of the voltage circuit), are reported in [20].

The AC losses were first measured using the conventional rectangular configuration for the voltage signal; after that, the measurements were repeated by setting the same operating parameters, but using the alternative arrangement described in the previous sections. Different values of α were tested in the rectangular arrangement: $3/2\,w$, $3\,w$, $7\,w$ and $11\,w$. Fig. 6a shows an image of this configuration, with $\alpha = 3\,w$.

In the alternative arrangement, both voltage taps are soldered as close as possible to the tape middle axis, so as to apply the correction term η_a corresponding to the central plateau region. An image of this setup is displayed in Fig. 6b. C_2 is placed on top of C_1, in order to replicate its shape as much as possible; therefore, in the figure they are not easily distinguishable.

In the following, when the dependency on the amplitude of the transport current is analysed, the average power dissipation over a full cycle is presented in terms of W/m. Instead, when the loss dependency on frequency is investigated, the overall losses per cycle are displayed in units of J/m.
The experimental data are compared with the results obtained through the abovementioned numerical model. Furthermore, the losses obtained with the well-known *Norris'* analytic formulation for a thin strip are also presented [62].

Fig. 7 shows the average power dissipation when the frequency of the transport current is set to 50 Hz, and I_m is varied. Fig. 7a displays the experimental results before the introduction of the correction terms. The curves referring to the conventional configuration converge as α increases. For α greater than $3w$, the discrepancies between the curves become negligible. The converging experimental curves for the rectangular arrangement are in agreement with both the numerical and analytic curves, especially at high current amplitudes.
The experimental curve referring to the alternative configuration presents values which are remarkably lower than the other curves, despite its trend is qualitatively similar. Furthermore, this discrepancy decreases as the current amplitude increases: compared to the numerical curve, its values are more than 20 times lower when $I_m = 0.35$, but only 2 times lower when $I_m = 0.85$.
Fig. 7b presents the same experimental results, after the correction by means of the correction terms. The curves referring to
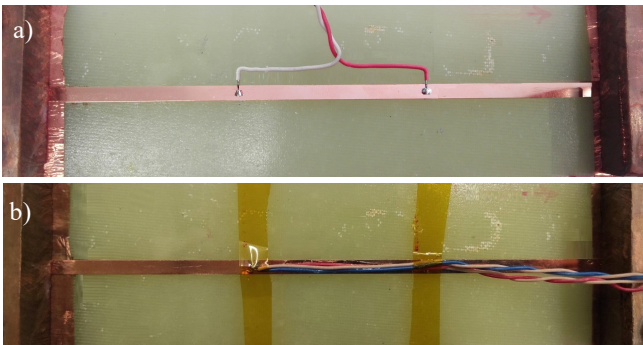
the conventional arrangement are in excellent agreement with the reference losses when $I_m > 0.4$, including the curve for $\alpha = 3/2\,w$, in which η_c has the greatest impact in reducing the measurement results. For the other curves, their variation compared to Fig. 7a cannot be noted in a logarithmic scale.
For what concerns the measurements carried out with the alternative configuration, they are much closer to the other curves when the correction term η_c is included. The curve is now only 1.25 times lower when $I_m = 0.35$, and 1.45 times higher when $I_m = 0.85$, compared to the reference losses. As expected, the correction due to η_c increases the measured values. The enhancement results slightly excessive for high current amplitudes, and this could be due to an incorrect determination of the value of β.
Moreover, both the curves with $\alpha = 3/2\,w$ and the one obtained with the alternative arrangement appear to diverge from the other curves when $I_m < 0.4$. This might be mainly ascribed to the difficulties in the correct acquisition of very small voltage signals at $I_m \ll I_c$, that might affect the measurement results.

Fig. 8 shows the transport current AC losses when I_m is set to 0.75, and the frequency is varied.
Before the introduction of the correction terms (Fig. 8a), the experimental curves obtained with the conventional arrangement converge to each other, already at $\alpha = 3w$. The discrepancies are minimal, as the ordinate axis is in linear scale. The curve found for $\alpha = 3/2\,w$ is the only one not converging, with

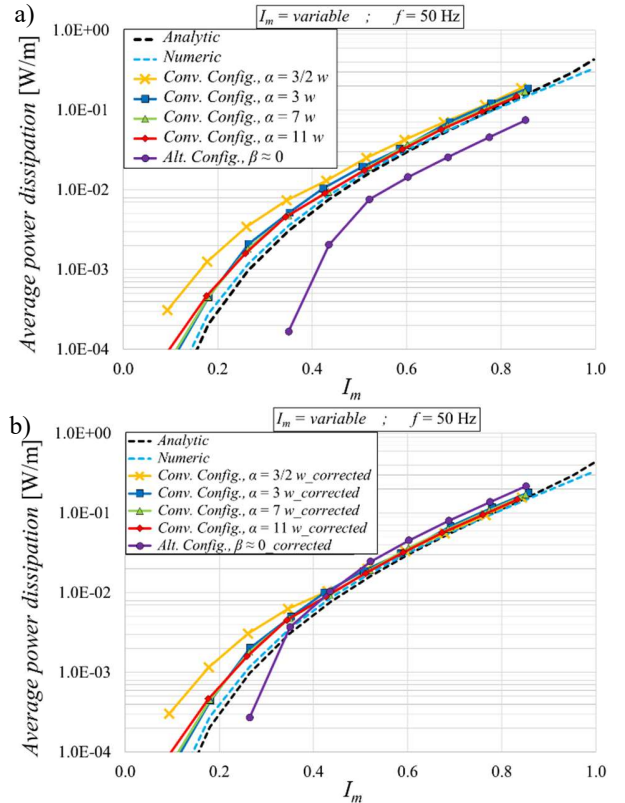Fig. 7. Average power dissipation in the *SuNAM SCN04* tape due to an AC transport current, measured in different experimental configurations, (a) before and (b) after the corrections with the parameters η_c and η_a. The frequency is set to 50 Hz and I_m is varied. The figures are in semi-logarithmic scale.

Fig. 6. Photo of the (a) conventional and (b) the alternative voltage measurement arrangement.

values at most 10% higher than the other curves. The trend of the experimental curves is in agreement with the numerical results, as well as with other similar works reported in the literature [63, 64].

They decrease almost linearly with increasing frequency, with a slope similar to that predicted by the numerical model. The crossing point with the analytical curve, which is frequency independent as it is computed under the assumptions of the critical state model adopted in *Norris*' formula, is around 200 Hz. On the other hand, the measurement results obtained with the alternative configuration correspond to about half of those referring to the other experimental curves.

As expected, the convergence between the experimental curves improves when applying the corrections, as shown in Fig. 8b. The impact of the parameter η_c is greater for the curve with $\alpha = 3/2\ w$, for which the correction determines slightly overestimated results. The corrected values are between 5 % lower to 10% higher than the other converging curves, due to possible experimental errors. The crossing frequency with the analytical curve moves towards smaller values, approaching the standard frequencies of power transmission grids. This is consistent with the results reported in [64] for tapes subjected to an AC transport current with similar I_m. As for the experimental curve referring to the alternative arrangement, the introduction of the

parameter η_a greatly improves its convergence, as the discrepancies are now included between 7% and 20% as compared to the other curves. Even in this case, the correction seems to slightly overestimate the losses at high transport currents.

V. Conclusion

This work presents a comprehensive investigation on the accuracy of the electrical measurement of AC losses due to sinusoidally varying transport currents in HTS coated conductors. A fully consistent theoretical treatment of the difference between the voltage measured with a voltmeter and the one actually needed for the calculation of AC losses is provided. The investigation of the measurement accuracy is carried out by determining a suitable correction term to be applied to the experimental data. The equations to evaluate this correction term are reported step-by-step, and numerically implemented for in relevant case studies. The novel algorithm allows one to *quantify* the impact of different measurement circuit configurations on the losses.

The results obtained for the configuration for electrical measurements based on a rectangular loop, widely adopted in the scientific community, show that increasing the distance from the tape middle axis at which the voltage taps are twisted together, the measurements converge to the expected AC losses. At a distance equal to 3 times the tape half-width, the losses become independent of the configuration. This threshold distance was already mentioned in previous papers, but with some discrepancies in the value of the distance itself, maybe due to the fact that its determination was mainly based on experimental observations. The present treatment allows a thorough quantitative assessment of this rule of thumb reported in the literature.

Given that the conventional arrangement requires a certain area of the measurement loop, which determines the linkage of flux due to electromagnetic noise, an alternative configuration is proposed here to tackle this issue. The proposed arrangement involves the use of an auxiliary measurement circuit, with short-circuited wires not soldered to the tape. The correction term for this alternative arrangement depends on the distance between the location of the voltage taps and the tape middle axis. There exists a unique point on the surface of the coated conductor, at which the measurement results coincide with the actual losses in the tape. However, meeting this particular condition is not trivial, as it requires a high accuracy in the soldering and might be impractical to achieve. In fact, small deviations from this position can determine significant errors, since the correction term varies abruptly around its null point. It is therefore preferable to solder the voltage taps close to the middle of the tape width, thus profiting of a central region in which the impact of the circuit arrangement is nearly constant, even though the magnitude of the correction is significant.

A dedicated experimental campaign was conducted on a SuNAM GdBCO tape, at different amplitudes and frequencies of the transport current. The losses obtained with different experimental configurations were compared with the results of the novel algorithm and existing analytical formulae. The results
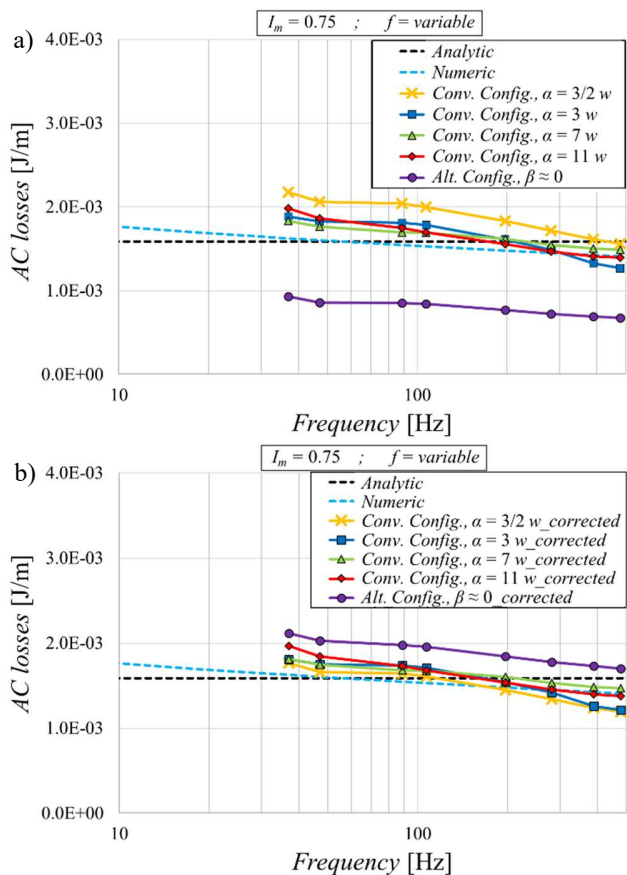

Fig. 8. Transport current AC losses in the *SuNAM SCN04* tape, measured in different experimental configurations, (a) before and (b) after the corrections with the parameters η_c and η_a. I_m is set to 0.75 and the frequency is varied. The figures are in logarithmic scale.

confirmed that, after the introduction of the correction terms, the measurements realized with different configurations converge with each other and with the computed losses, especially for current amplitudes greater than 40% of the tape critical current. It is experimentally proved that the AC losses converge to a reference value adopting the conventional measurement configuration, when the distance from the tape middle axis at which the voltage taps are twisted together is equal or greater than 3 times the tape half-width. Moreover, after correction, the curve referring to the alternative arrangement gives results which are slightly higher than the other curves, probably due to inaccuracies in the positioning of the voltage taps. Thus, it is recommended to limit the application of the proposed alternative configuration to specific cases in which the electromagnetic noise would excessively affect the measurement results. Otherwise, the conventional rectangular loop arrangement should be preferred.

Future developments will consist in applying the proposed algorithm to generate standard scaling methods. This could allow the identification of empirical formulae, obtained by fitting the numerical results, to compute correction factors suited to treat multiple datasets (different tapes and operating conditions) without requiring the availability of numerical codes.

VI. APPENDIX

The complete expression of the mean value in a period T of the power dissipated in the tape due to the non-conservative component of the electric field, which appears in *Section* II is:

$$
\begin{aligned}
&\langle p_A(t) \rangle = \\
&= \frac{1}{T} \int_0^T \left\{ -L_0 \int_{-\frac{\delta}{2}}^{\frac{\delta}{2}} \int_{-w}^{w} \frac{\partial A}{\partial t}(x,y,t) J_i(t)\, dx\, dy \right\} dt
\end{aligned} \tag{A.1}
$$

Then, the vector potential can be expressed as follows:

$$
\begin{aligned}
&A(x,y,t) = \\
&= \frac{\mu_0}{4\pi} \int_{-\frac{L}{2}}^{\frac{L}{2}} \int_{-w}^{w} \int_{-\delta}^{\frac{\delta}{2}} \frac{J(x',y',t)}{d(x,y,0,x',y',z')}\, dz' dy' dx'
\end{aligned} \tag{A.2}
$$

Considering (A.2) and (A.1) yields:

$$
\begin{aligned}
&\langle p_A(t) \rangle = -\frac{\mu_0 L_0}{4\pi T} \int_0^T \left\{ \int_{-\frac{\delta}{2}}^{\frac{\delta}{2}} \int_{-w}^{w} \int_{-\frac{L}{2}}^{\frac{L}{2}} \int_{-\frac{\delta}{2}}^{\frac{\delta}{2}} \int_{-w}^{w} \right. \\
&\left. \frac{\frac{\partial J}{\partial t}(x',y',t) J(x,y,t)}{d(x,y,0,x',y',z')}\, dx' dy' dz' dx\, dy \right\}
\end{aligned} \tag{A.3}
$$

where the term at the denominator $d(x,y,z,x',y',z') = \sqrt{(x-x')^2 + (y-y')^2 + (z-z')^2}$ represents the module of the distance between the *field point* (x,y,z) and the *source point* (x',y',z'). Moreover, considering the expression of the time derivative of the product of two functions, yields:

$$
\begin{aligned}
&\frac{\partial J}{\partial t}(x',y',t) J(x,y,t) = \\
&= \frac{\partial}{\partial t}[J(x',y',t) J(x,y,t)] - J(x',y',t) \frac{\partial J}{\partial t}(x,y,t)
\end{aligned} \tag{A.4}
$$

Introducing (A.4) into (A.3) gives:

$$
\begin{aligned}
&\langle p_A(t) \rangle = -\frac{\mu_0 L_0}{4\pi T} \int_0^T \left\{ \int_{-\frac{\delta}{2}}^{\frac{\delta}{2}} \int_{-w}^{w} \int_{-\frac{L}{2}}^{\frac{L}{2}} \int_{-\frac{\delta}{2}}^{\frac{\delta}{2}} \int_{-w}^{w} \right. \\
&\left. \frac{\frac{\partial}{\partial t}[J(x',y',t) J(x,y,t)]}{d(x,y,0,x',y',z')}\, dx' dy' dz' dx\, dy \right\} dt \\
&+ \frac{\mu_0 L_0}{4\pi T} \int_0^T \left\{ \int_{-\frac{\delta}{2}}^{\frac{\delta}{2}} \int_{-w}^{w} \int_{-\frac{L}{2}}^{\frac{L}{2}} \int_{-\frac{\delta}{2}}^{\frac{\delta}{2}} \int_{-w}^{w} \right. \\
&\left. \frac{J(x',y',t) \frac{\partial J}{\partial t}(x,y,t)}{d(x,y,0,x',y',z')}\, dx' dy' dz' dx\, dy \right\} dt
\end{aligned} \tag{A.5}
$$

Switching the order in which the space and time integrals are performed in the first term at the r.h.s. in (A.5), the time integral can be solved first. This integral is null and the whole term is canceled out given that the regime is sinusoidal. Furthermore, both (A.3) and (A.5) have the same term at the l.h.s.; consequently, the r.h.s. of both equations are equal. Changing the integration order in (A.5) yields:

$$
\begin{aligned}
&-\frac{\mu_0 L_0}{4\pi T} \int_0^T \left\{ \int_{-\frac{L}{2}}^{\frac{L}{2}} \left[\int_{-\frac{\delta}{2}}^{\frac{\delta}{2}} \int_{-w}^{w} \int_{-\frac{\delta}{2}}^{\frac{\delta}{2}} \int_{-w}^{w} \frac{\frac{\partial J}{\partial t}(x',y',t) J(x,y,t)}{d(x,y,0,x',y',z')} \right. \right. \\
&\left. \left. dx' dy' dx\, dy \right] dz' \right\} dt = \frac{\mu_0 L_0}{4\pi T} \int_0^T \left\{ \int_{-\frac{L}{2}}^{\frac{L}{2}} \left[\int_{-\frac{\delta}{2}}^{\frac{\delta}{2}} \int_{-w}^{w} \int_{-\frac{\delta}{2}}^{\frac{\delta}{2}} \int_{-w}^{w} \right. \right. \\
&\left. \left. \frac{J(x',y',t) \frac{\partial J}{\partial t}(x,y,t)}{d(x,y,0,x',y',z')}\, dx' dy' dx\, dy \right] dz' \right\}
\end{aligned} \tag{A.6}
$$

Then, it can easily be proved that in the terms at the denominator of (A.6) it is possible to exchange the *source points* and the *field points*. Moreover, considering that the integration extremes for both *source points* and *field points* are equal, a change of variable is performed only on the l.h.s. of (A.6): y' is substituted with y, and x' is substituted with x. Thus, the l.h.s. of (A.6) can be reformulated as:

$$
\begin{aligned}
&-\frac{\mu_0 L_0}{4\pi T} \int_0^T \left\{ \int_{-\frac{L}{2}}^{\frac{L}{2}} \left[\int_{-\frac{\delta}{2}}^{\frac{\delta}{2}} \int_{-w}^{w} \int_{-\frac{\delta}{2}}^{\frac{\delta}{2}} \int_{-w}^{w} \frac{J(x',y',t) \frac{\partial J}{\partial t}(x,y,t)}{d(x,y,0,x',y',z')} \right. \right. \\
&\left. \left. dx' dy' dx\, dy \right] dz' \right\} dt
\end{aligned} \tag{A.7}
$$

Substituting (A.7) as the l.h.s. of (A.6), it turns out that both sides of the resulting equation are equal except for their sign. For the equation to be correct, the only possible solution corresponds to having both sides equal to zero. If this is the case, it follows that the r.h.s. of (A.3) is null, which confirms that $\langle p_A(t) \rangle = 0$.

REFERENCES

[1] F. Grilli and S. P. Ashworth, "Measuring transport AC losses in YBCO-coated conductor coils," *Supercond. Sci. Technol.,* vol. 20, pp. 794–799, Jun. 2007.

[2] F. Gomory *et al.,* "AC losses in coated conductors," Supercond. Sci. Technol., vol. 23, p. 034012, Feb. 2010.

[3] F. Grilli *et al.,* "Computation of Losses in HTS Under the Action of Varying Magnetic Fields and Currents", *IEEE Trans. Appl. Supercond.*, vol. 24, no. 1, pp. 78–110, Feb. 2014.

[4] F. Grilli and A. Kario, "How filaments can reduce AC losses in HTS coated conductors: a review," *Supercond. Sci. Technol.*, vol. 29, p. 083002, Jul. 2016.

[5] B. Shen *et al.,* "Investigation and comparison of AC losses on stabilizer-free and copper stabilizer HTS tapes," *Phys. C: Superconductivity and its applications*, vol. 471, pp. 40–44, Aug. 2017.

[6] R. Pei *et al.,* "High-precision digital lock-in measurements of critical current and AC loss in HTS 2G-tapes", *2008 SICE Annual Conference*, pp. 3147–3150, 2008.

[7] S. P. Ashworth and M. Suenaga, "Local calorimetry to measure ac losses in HTS conductors," *Cryogenics.,* vol. 41, pp. 77–89, Feb. 2001.

[8] M. Yagi *et al.,* "Measurement of AC Losses of Superconducting Cable by Calorimetric Method and Development of HTS Conductor With Low AC Losses", *IEEE Trans. Appl. Supercond.,* vol. 13, no. 2, pp. 1902–1905, Jun. 2003.

[9] K. W. See *et al.,* "Innovative Calorimetric AC Loss Measurement of HTSC for Power Applications", *IEEE Trans. Appl. Supercond.*, vol. 21, no. 3, pp. 3261 - 3264, Jun. 2011.

[10] J. P. Murphy *et al.,* "Experiment Setup for Calorimetric Measurements of Losses in HTS Coils Due to AC Current and External Magnetic Fields", *IEEE Trans. Appl. Supercond.*, vol. 23, no. 3, p. 4701505, Jun. 2013.

[11] Y. Yang *et al.,* "Configuration and calibration of pickup coils for measurement of ac loss in long superconductors", *J. Appl. Phys.*, vol. 96. no. 4, pp. 2141–2149, Aug. 2004.

[12] N. Amaro *et al.,* "Contactless Loop Method for Measurement of AC Losses in HTS Coils", *IEEE Trans. Appl. Supercond.*, vol. 25, no. 3, p. 9000604, Jun. 2015.

[13] Y. Wang *et al.,* "Review of AC Loss Measuring Methods for HTS Tape and Unit", *IEEE Trans. Appl. Supercond.*, vol. 24, no. 5, p. 9002306, Oct. 2014.

[14] S. Safran *et al.,* "AC loss characterization of single pancake BSCCO coils by measured different methods," *Phys. C: Superconductivity and its applications*, vol. 541, pp. 45–49, Aug. 2017.

[15] D. N. Nguyen *et al.,* "Electrical measurements of AC losses in high temperature superconducting coils at variable temperatures," *Supercond. Sci. Technol.*, vol. 26, p. 095001, Jul. 2013.

[16] J. Kim *et al.,* "Transport AC Loss Measurements in Superconducting Coils", *IEEE Trans. Appl. Supercond.*, vol. 21, no. 3, pp. 3269–3272, Jun. 2011.

[17] S. K. Olsen *et al.*, "Alternating current losses of a 10 metre long low loss superconducting cable conductor determined from phase sensitive measurements", *Supercond. Sci. Technol.*, vol. 12, no. 6, pp. 360–365, Jun. 1999.

[18] B. Shen *et al.,* "Power dissipation in HTS coated conductor coils under the simultaneous action of AC and DC currents and fields", *Supercond. Sci. Technol.*, vol. 31, no. 7, p. 075005, Jul. 2018.

[19] J. Ogawa *et al.,* "Measurements of AC transport current losses in HTS tapes in an assembled conductor", *AIP Conference Proceedings,* vol. 411, no. 3, pp. 805–811, Jul. 2004.

[20] M. Breschi *et al.,* "An electromagnetic method for measuring AC losses in HTS tapes without lock-in amplifier," *J. of Phys.: Conference Series*, vol. 1559, no.1, p. 012066, Jun. 2020.

[21] M. Ciszek *et al.,* "Transport AC losses in multifilamentary Ag/Bi-2223 tapes in low external DC magnetic fields," *Phys. C*, vol. 272, pp. 319–325, Dec. 1996.

[22] T. Fukunga *et al.,* "Advances in Superconductivity VI," edited by *T. Fujita and Y. Shiohara (Springer, Tokyo, 1994)*, pp. 633–636.

[23] A. M. Campbell, "AC Losses in High T_c Superconductors", *IEEE Trans. Appl. Supercond.*, vol. 5, no. 2, pp. 682–687, Jun. 1995.

[24] Y. Yang *et al.,* "The influence of geometry on self-field AC losses of Ag sheathed PbBi2223 tapes," *Phys. C*, vol. 256, pp. 378–386, Feb. 1996.

[25] J. R. Clem et al., "Voltage-probe-position dependence and magnetic-flux contribution to the measured voltage in ac transport measurements: Which measuring circuit determines the real losses?" *Recent Developments in High Temperature Superconductivity. Lecture Notes in Physics*, vol. 475, pp. 253–264, 1996.

[26] S. Fleshler *et al.,* "Measurement of the ac power loss of (Bi,Pb)2Sr2Ca2Cu3Ox composite tapes using the transport technique," *Appl. Phys.*, vol. 67, no. 21, Lett, pp. 3189–3191, Nov. 1995.

[27] M. Ciszek *et al.,* "The effect of potential contact position on AC loss measurements in superconducting BSCCO tape," *Phys. C*, vol. 233, pp. 203–208, Nov. 1994.

[28] J. R. Clem *et al.,* "Penetration of Magnetic Flux and Electrical Current Density into Superconducting Strips and Disks," *Chinese Journal of Physics*, vol. 34, no. 2–11, pp. 284–290, Apr. 1996.

[29] S. A. Awan *et al.,* "Self-field a.c. losses in filamentary Bi2223/Ag frequencies," *Cryogenics*, vol. 37, no. 10, pp. 633–635, 1997.

[30] L. Jansak *et al.* "Critical current anisotropy and AC losses in Bi(Pb)SrCaCu0-2223 and TlBaCaCuO- 2212 Ag sheathed superconducting tapes," *IEEE Trans. Magn .* vol. 32, no. 4, pp. 2788–2791, Jul. 1996

[31] M. Ciszek *et al.,* "Energy dissipation in high temperature ceramic superconductors," *Appl. Supercond.*, vol. 3, no. 7–10, pp. 509–520, Oct. 1995.

[32] C. Beduz et al., "A series of round-robin measurements of the self-field ac loss of Bi-2223 tapes," *Supercond. Sci. Technol.,* vol. 11, pp. 675–679, 1998.

[33] H. Eckelmann *et al.,* "AC transport current losses of multifilamentary Bi2223/ tapes with varying filament geometries," *Phys. C.,* vol. 295, pp. 198–208, Feb. 1998.

[34] J. J. Rabbers *et al.,* "Self-field loss of BSCCOrAg tape in external AC magnetic field," *Phys. C.,* vol. 300, no.1–2, pp. 1–5, May. 1998.

[35] O. Tsukamoto *et al.,* "Measurements of AC Transport Current Losses in HTS Tapes in an Assembled Conductor", *IEEE Trans. Appl. Supercond.*, vol. 15, no. 2, pp. 2895–2898, Jun. 2005.

[36] B. Klincok et al., "The voltage signal on a superconducting wire in AC transport," *Supercond. Sci. Technol.,* vol. 18, pp. 694–700, Apr. 2005.

[37] J. Ogawa *et al.,* "Measurement of total AC losses in HTS short sample wires by electric and calorimetric methods," *AIP Conference Proceedings* vol. 711, pp. 805–811, Jun. 2004.

[38] Y. Wang *et al.,* "An applicable calorimetric method for measuring AC losses of 2G HTS wire using optical FBG," *Science China Technological Sciences,* vol. 58, pp. 545–550, Jan. 2015.

[39] S. Fukui *et al.,* "Transport Current AC Losses of High-Tc Superconducting Tapes Exposed to AC Magnetic Field," *Advances in Cryogenic Engineering Materials*, vol. 44, pp. 723–730, 1998.

[40] J. Ogawa *et al.,* "Comparison between experimental and numerical analysis of AC transport current loss measurement in YBCO tapes in an assembled conductor," *Phys. C*, vol. 445–448, pp. 1083–1087, Jun. 2006.

[41] Z. Jiang *et al.,* "The dependence of AC loss characteristics on the space in stacked YBCO conductors", *Supercond. Sci. Technol.*, vol. 21, p. 015020, Dec. 2007.

[42] J. Ogawa *et al.,* "Influence of Transport Current Distribution on AC Transport Current Loss Measurement in an Assembled Conductor," *IEEE Trans. Appl. Supercond*, vol. 20, no. 3, pp. 1300–1303, Jun. 2010.

[43] Z. Jiang *et al.,* "Comparison of transport AC losses in an eight-strand YBCO Roebel cable and a four-tape YBCO stack," *Phys. C*, vol. 471, no. 21–22, pp. 999–1002, Nov. 2011.

[44] P. Zhou *et al.,* "Transition frequency of transport ac losses in high temperature superconducting coated conductors", *J. Appl. Phys.*, vol. 126, no. 6, p. 063901, Aug. 2019.

[45] J. J. Rabbers *et al.,* "Advanced ac loss measurement methods for high-temperature superconducting tapes," *Review of Scientific Instruments*, vol. 72, pp. 2365–2372, Feb. 2001.

[46] M. Vojenciak *et al.,* "Influence of the voltage taps position on the self-field DC and AC transport characterization of HTS superconducting tapes," *Cryogenics.*, vol. 57, pp. 189–194, Aug. 2013.

[47] M. Ciszek *et al.,* "Effect of the Neighboring Tape's AC Currents on Transport Current Loss of a Bi-2223 Tape," *IEEE Trans. Appl. Supercond.*, vol. 11, no. 1, pp. 2220–2223, Mar. 2001.

[48] S. Choi *et al., "*AC transport current loss in stacked HTS tapes," *Phys. C.*, vol. 372–376, pp. 1746–1749, Aug. 2002.

[49] E. H. Brandt, "Thin superconductors in a perpendicular magnetic AC field: General formulation and strip geometry," *Phys. Rev. B*, vol. 49, no. 13, pp. 9024–9040, 1994.

[50] A. Musso *et al,* "Analysis of AC Loss Contributions From Different Layers of HTS Tapes Using the A−V Formulation Model," *IEEE Trans. on Appl. Supercond.,* vol. 31, no. 2, p. 5900411, Mar. 2021.

[51] N. Amemiya *et al.*, "Numerical modelings of superconducting wires for AC loss calculations," *Physica C.*, vol. 310, issue 1–4, pp. 16–29, Dec. 1998.

[52] E. Vinot *et al.* "Different Formulations to Model Superconductors*," IEEE Trans. On Appl. Supercond.*, vol. 36, no. 4, pp. 1226–1229, Jul. 2000.

[53] F. Grilli *et al.*, "Finite-Element Method Modeling of Superconductors: From 2-D to 3-D," *IEEE Trans. On Appl. Supercond.*, vol. 15, no. 1, pp. 17–24, Mar. 2005.

[54] F. Grilli, "Numerical Modeling of HTS Applications*," IEEE Trans. On Appl. Supercond.*, vol. 26, no. 3, p. 0500408, Apr. 2016.

[55] S. Otten *et al.*, "Simple and Fast Method for Computing Induced Currents in Superconductors Using Freely Available Solvers for Ordinary Differential Equations," *IEEE Trans. On Appl. Supercond*, vol. 29, no.8, p. 8202008, Dec. 2019.

[56] N. C. Allen *et al.*, "Numerical and experimental investigation of the electromechanical behavior of rebco tapes," *IOP Conf. Ser.: Mater. Sci. Eng.*, vol. 102, p. 012025, 2015.

[57] B. Shen *et al.*, "Overview of H-Formulation: A Versatile Tool for Modeling Electromagnetics in High-Temperature Superconductor Applications," *IEEE Access*, vol. 8, pp. 100403–100414, May 2020.

[58] B. Shen *et al., "*Review of the AC loss computation for HTS using H formulation," *Supercond. Sci. Technol*., vol. 33, no. 3, p. 033002, Feb. 2020.

[59] *S. Stavrev et al., "*Comparison of numerical methods for modeling of superconductors," *IEEE Trans. Magn., vol. 38, no. 2, pp. 849–852, Mar. 2002.*

[60] H. Tonsho *et al.,* "Theoretical and experimental study on AC loss in HTS tape in AC magnetic field carrying AC transport current," *IEEE Trans. Appl. Supercond., vol. 13, no. 2, pp. 2368–2371, Jun. 2003.*

[61] *M. Vojenciak et al.,* "Losses in Bi-2223/Ag tape at simultaneous action of AC transport and AC magnetic field shifted in phase," *J. Phys. Conf. Ser., vol. 43, pp. 63–66, Sep. 2005.*

[62] W. T. Norris, "Calculation of hysteresis losses in hard superconductors carrying AC isolated conductors and edges of thin sheets," *J. Phys. Appl. Phys.*, vol. 3, no. 4, pp. 489–507, Apr. 1970.

[63] K. P. Thakur *et al.*, "Frequency-dependent critical current and transport ac loss of superconductor strip and Roebel cable*," Supercond. Sci. Technol.*, vol. 24, no. 6, Apr. 2011.

[64] F. Sirois *et al.*, "Comparison of Constitutive Laws for Modeling High-Temperature Superconductors," *IEEE Trans. On Appl. Supercond.*, vol. 29, no. 1, Jan. 2019.

Marco Breschi graduated with honors in Electrical Engineering from the University of Bologna, Italy, in July 1997. He received his Ph.D. in Electrical Engineering from the University of Bologna in March 2001, with a study on the electrodynamics of superconducting magnets for the Large Hadron Collider of CERN. In 2004 he worked as a visiting scientist at the National High Magnetic Field Laboratory, Florida, USA. Since October 2001 he is Assistant Professor, and since October 2014 he is Associate Professor at the Department of Electrical, Electronic and Information Engineering of the University of Bologna. His research activity is related to various aspects of magnet technology, applied superconductivity and the numerical computation of electromagnetic fields. He is the author or co-author of several multiphysics models for superconducting wires, cables and magnets, based either on FEM or circuit models, developed to investigate the electromagnetic, electrothermal, and electromechanical phenomena of interest for technical applications. From 2007 to 2017 he was an independent member of the Working Group SULTAN of ITER (International Thermonuclear Experimental Reactor) and coordinated several research projects for the analysis of the ITER cable in Conduit Conductors performance. From 2013 to 2015 he served as a Chairman of the IOC of the CHATS-AS Workshop on numerical modeling of superconducting devices. In 2019 he was appointed Co-Chairman of the European Conference on Applied Superconductivity (EUCAS) to be held in Bologna, Italy, in 2023.

Andrea Musso graduated with honors in Energy Engineering from the University of Bologna, Italy, in March 2017. He received his Ph.D. in Electrical Engineering from the University of Bologna in June 2021, with a study on the electrodynamic transients in High Temperature Superconducting (HTS) tapes and coils. In 2016/17, he worked as a trainee at the TE-MSC group at CERN, Switzerland. In 2020, he spent a semester at the Applied Superconductivity Lab of Seoul National University, Republic of Korea, as a visiting student and researcher. His main research interests are related to the magnetic application of high and low temperature superconductors. He dealt with transient operations of HTS tapes and No-Insulation coils, with pancake-wound and layer-wound techniques, developing FEM and circuit models, as well as experimental activities for the electric measurement of AC losses. Nowadays, he is a Post Doc researcher at his Alma Mater, carrying out a technical-economic analysis of electric transmission HTS cables, for use in the electricity grid.

Gaetano Pasini (IEEE Member since 1997) received the degree in Electronic Engineering from the University of Bologna, Bologna, Italy, in 1991. He joined the Electrical and Electronic Measurement Group, Electrical Engineering Department, University of Bologna, as an Assistant Professor, in 1993, where he was an Associate Professor in 2001. He was a co-founding partner with TechImp HQ SpA, Bologna, Italy, from 1999 to 2009, where he was involved in design tools and algorithms for medium and high voltage devices diagnostic. His current research interests include digital-signal processing, nonconventional-sampling strategies, modeling and characterization of nonlinear devices, distributed measurement systems, and impedance measurements on superconductors.

Pier Luigi Ribani took his degree in Nuclear Engineering at the University of Bologna on October 1982. He was graduated technician at the Department of Electrical Engineering of the University of Bologna from 1987 to 1990 and researcher, in the same Department, from 1990 to 1998. Since 1998 he is associate professor at the Department of Electrical Engineering. His main research activity includes the modelling of electromagnetic systems and devices and applied superconductivity. He was involved in many national and international research projects. In particular, he participated, in cooperation with researchers of University of Udine and Politecnico di Torino, to the development of code THELMA for the analysis of LTS cables for controlled thermonuclear fusion experiments. He was involved, in cooperation with the superconductivity group at the Department of Electrical Engineering of the University of Bologna, in the design and analysis of many superconducting devices for power applications, in particular SMES and FCL.